



BASIC SCIENCE ARTICLE

Increased antioxidant response in medium-chain acyl-CoA dehydrogenase deficiency: does lipoic acid have a protective role?

Zahra Nochi¹, Rune Isak Dupont Birkler¹, Paula Fernandez-Guerra¹, Jakob Hansen², Flemming Wibrand³, Thomas Juhl Corydon^{4,5}, Niels Gregersen¹ and Rikke Katrine Jentoft Olsen¹

BACKGROUND: Medium-chain acyl-CoA dehydrogenase (MCAD) deficiency (MCADD) is the most frequent fatty acid oxidation (FAO) defect in humans. MCAD-deficient fibroblasts are more resistant to oxidative stress-induced cell death than other FAO defects and healthy controls.

METHODS: Herein we investigate the antioxidant response and mitochondrial function in fibroblasts from MCAD-deficient patients (c.985 A>G/c.985 A>G) and healthy controls.

RESULTS: MCAD-deficient fibroblasts showed increased level of mitochondrial superoxide, while lipids were less oxidatively damaged, and higher amount of manganese superoxide dismutase were detected compared to healthy controls, showing forceful antioxidant system in MCADD. We showed increased maximal respiration and reserve capacity in MCAD-deficient fibroblasts compared to controls, indicating more capacity through the tricarboxylic acid (TCA) cycle and subsequently respiratory chain. This led us to study the pyruvate dehydrogenase complex (PDC), the key enzyme in the glycolysis releasing acetyl-CoA to the TCA cycle. MCAD-deficient fibroblasts displayed not only significantly increased PDC but also increased lipoylated PDC protein levels compared to healthy controls.

CONCLUSIONS: Based on these findings, we raise the interesting hypothesis that increased PDC-bound lipoic acid, synthesized from accumulated octanoic acid in MCADD, may affect the cellular antioxidant pool in MCADD.

Pediatric Research (2020) 88:556–564; <https://doi.org/10.1038/s41390-020-0801-1>

INTRODUCTION

Mitochondrial fatty acid oxidation (FAO) disorders, a group of frequent inborn errors of metabolism, result from genetic defects in transport proteins or enzymes involved in mitochondrial fatty acid β -oxidation. The most common FAO disorder is characterized by a deficiency of medium-chain acyl-CoA dehydrogenase (MCAD) activity, which is due to pathogenic variations in the *ACADM* gene. MCAD deficiency (MIM# 201450) is autosomal recessively inherited and usually presents in the first years of life. The prevalent disease-causing variation is c.985 A>G, which results in replacement of a lysine by a glutamate at position 329 of the precursor protein (p. Lys329Glu).¹ Inherited MCAD deficiency can be asymptomatic or show severe consequences, such as metabolic acidosis, hypoketotic hypoglycemia, vomiting, seizures, and lethargy, which may progress to coma and sudden death.² Milder symptoms include developmental delay, myopathy, and hypotonia.³ The resulting variant protein of the c.985 A>G mutation is prone to misfolding, which may lead to premature degradation and/or aggregation, and the disorder is categorized as a protein misfolding disease.⁴ MCAD deficiency impairs the body's ability to metabolize medium-chain fatty acids into acetyl-CoA and subsequently convert it to energy through activity of the tricarboxylic acid (TCA) cycle, coupled to oxidative phosphorylation in the respiratory chain. The enzymatic

defect is easily indicated by detection of the characteristic metabolites, especially octanoyl- and decanoyl-carnitine in the blood using tandem mass spectrometry (MS/MS).⁵ Besides energy deficiency, MCAD deficiency, like other metabolic disorders, has underlying pathophysiological mechanisms related to reactive oxygen species (ROS) production.⁶ The source of ROS in MCADD is not known. However, accumulated substrates (octanoic acid and decanoic acid) due to misfolding or lacking MCAD protein have been suggested to play a role.^{7–9} ROS affects the permeability of the blood–brain barrier, enhancing neuronal vulnerability to ROS toxicity. However, compared to other FAO defects and healthy controls, fibroblasts from MCAD-deficient patients have been shown to be more resistant to oxidative stress, and less muscular and neural damage were observed.¹⁰

In the present study, we investigated the antioxidant response and mitochondrial function in cultured MCAD-deficient skin fibroblasts as compared to healthy controls.

METHODS

Cell culturing

Three dermal fibroblast cultures (P1–P3) from three unrelated patients with MCAD deficiency were included in the study. The

¹Research Unit for Molecular Medicine, Department of Clinical Medicine, Aarhus University Hospital and Faculty of Health, Aarhus University, Aarhus, Denmark; ²Department of Forensic Medicine, Aarhus University, Aarhus, Denmark; ³Department of Clinical Genetics, Rigshospitalet, Copenhagen, Denmark; ⁴Department of Biomedicine, Aarhus University, Aarhus, Denmark and ⁵Department of Ophthalmology, Aarhus University Hospital, Aarhus, Denmark
Correspondence: Zahra Nochi (z.nochi@clin.au.dk)

Received: 2 April 2019 Revised: 30 September 2019 Accepted: 7 December 2019

Published online: 11 February 2020

MCAD-deficient patient fibroblasts had the following homozygous genotype: *ACADM* c.985 A>G, and all three healthy controls (Promocell #c-12300 # 102402.2, Promocell #c-12300 #2090402, and ATCC #CRL-2450) were homozygous for the wild-type sequence. According to approval and regulations from the Danish Ethical Committee, the patient fibroblasts were de-identified.

The fibroblasts were incubated at 37 °C and humidified atmosphere of 5% (v/v) CO₂ in Roswell Park Memorial Institute (RPMI)-1640 medium (Fischer Scientific, Hampton, NH) supplemented with 2 mmol/L of L-glutamine (Sigma Aldrich, St. Louis, MO), 10% fetal calf serum (Sigma Aldrich), and 1% penicillin/streptomycin (Sigma Aldrich).

Acylcarnitine profiling

Control and patient fibroblasts were cultured in L-carnitine (0.4 mmol/L) enriched medium. The cell culture medium was harvested at sub-confluence and frozen at -20 °C. Twenty-five microliters of medium and 10 µL internal standard solution (containing deuterated acylcarnitines) were supplemented with acetonitrile to a total volume of 500 µL in an Eppendorf tube. The extraction mixture was vortexed and centrifuged for 10 min at 18,500 × *g*, and 200 µL of the supernatant was carefully transferred to a glass vial. A 10-µL sample aliquot was analyzed on a Waters ACQUITY™ ultra-performance liquid chromatographic system (Waters Corporation, Milford, MA) connected to a Waters TQS triple quadrupole mass spectrometer with electrospray ionization operating in positive ion mode.

Selected reaction monitoring (SRM) was used to monitor octanoyl- and decanoyl-carnitine with the following transitions: octanoyl-carnitine *m/z* = 288.2 → 85.0, octanoyl-carnitine-D₃ *m/z* = 291.2 → 85.1, decanoyl-carnitine *m/z* = 316.2 → 85.0, decanoyl-carnitine-D₃ *m/z* = 319.3 → 85.0. Separate calibrator samples containing 0.00125–1.25 µM octanoyl- and decanoyl-carnitine was prepared from dilutions of reference compound material using the same sample preparation procedure as specified for the cellular samples. Quantitative values were derived from linear regression analysis of calibrator samples using peak area ratios (analyte/internal standard) for each analyte.

All measurements were normalized to total protein amount after analysis using the Bradford protein assay (Bio-Rad, Hercules, CA), and mean values are expressed.

Mitochondrial superoxide levels by MitoSOX measurements

Mitochondrial superoxide levels were measured using the MitoSOX™ Red Mitochondrial Superoxide Indicator (Life Technologies, Carlsbad, CA). Measurements of cellular fluorescence were performed using the NucleoCounter® NC-3000 image cytometer (NC-3000) (Chemometec, Denmark) and analyzed according to Fernandez-Guerra et al.¹¹ with some modifications; we used SYTOX™ green (Life Technologies) nucleic acid stain to distinguish dead from live cells excited at 488 nm with emission in the 530/30 band pass filter.

Cellular lipid peroxidation (LPO) levels by BODIPY measurements The BODIPY® 581/591 undecanoic acid (BODIPY) (Life Technologies), an intrinsically lipophilic fluorophore, was used to measure the level of LPO. Once inside the cell, the polyunsaturated butadienyl portion of the dye is oxidized and results in a shift of the fluorescence emission peak from ~590 to ~510 nm. Cells at 80% confluence were incubated in RPMI-1640 containing BODIPY at 10 µmol/L for 30 min at 37 °C, washed twice with phosphate-buffered saline (PBS, pH 7.4), trypsinized, re-suspended in Hoechst 33342 at 10 µg/mL, and incubated for 15 min at 37 °C for nuclear staining. Measurements of cellular fluorescence were performed using the NC-3000. The settings of the NC-3000 used in this study consist of three different channels having excitation peak wavelengths at 365, 475, and 530 nm with emission filters at 470/55, 560/35, and 675/75 nm, respectively. Fluorescent image

acquisition, image analysis, subpopulation definition and quantification, and data visualization were performed with the NC-3000 software.

Mitochondrial bioenergetics profiling by Seahorse analyzer

Oxygen consumption rate (OCR) and extracellular acidification rate (ECAR) were measured using Seahorse XFe96 extracellular flux analyzer (Agilent Technologies, Santa Clara, CA) to profile mitochondrial bioenergetics parameters in cells. Control and patient fibroblasts were seeded at 15,000 cells/well in a Seahorse cell culture microplate and incubated overnight at 37 °C in a humidified atmosphere of 5% CO₂. Twenty-four hours later, on the day of analysis, cell culture medium was changed into Seahorse XF base medium (minimal Dulbecco's modified Eagle's medium) supplemented with 10 mmol/L glucose, 2 mmol/L glutamine, and 1 mmol/L sodium pyruvate (pH 7.4) followed by incubation at 37 °C in a non-CO₂ incubator for 1 h. The key parameters of mitochondrial respiration were measured using the Seahorse XF Cell Mito Stress Test Kit and analyzed according to Zhou et al.¹² (Fig. 3a). OCR and ECAR were automatically recorded and calculated by the Seahorse XFe96 software (Wave 2.3.0).

Protein extraction

Following pre-culturing, the cell cultures were transferred to 3 × 150 cm² culture flasks and harvested at sub-confluence by detaching in trypsin-EDTA solution and PBS (pH 7.4), centrifuged for 3 min at 405 × *g*, and washed twice in PBS. Cell lysis and protein extraction were performed according to Birkler et al.¹³

Mitochondrial manganese superoxide dismutase (MnSOD) levels by MS analysis

Extracted total cell proteins (20 µg) of all samples were separated by sodium dodecyl sulfate–polyacrylamide gel electrophoresis and processed as previously described.¹³ Mitochondrial SOD (MnSOD) levels along with β-actin as reference protein were measured using triple quadrupole mass spectrometer. Relative protein values were obtained using SRM MS analysis according to Birkler et al.¹³ β-Actin was chosen as the reference protein in order to have the same reference protein in the whole study.

Western blotting

Western blotting was performed as previously described¹⁴ with the following antibodies: (1) anti-DLAT (dihydrolipoamide S-acetyltransferase or PDC-E2) antibody (PA5-29043) (Thermo Fischer Scientific), diluted 1:5000 (detected at molecular weight (MW) 70 kDa), (2) anti-DBT (dihydrolipoamide branched-chain transacylase or BCKDC-E2) antibody (PA5-29727) (Thermo Fischer Scientific) diluted 1:500 (detected at MW 52 kDa), (3) anti-DLST (dihydrolipoamide succinyltransferase or KGDC-E2) antibody (PA5-22239) (Thermo Fischer Scientific), diluted 1:1000 (detected at MW 49 kDa), and (4) anti-lipoic acid antibody (437695) (Merck Millipore, Billerica, MA), diluted 1:2500 (detected at MW 70 and 49 kDa). For reference, β-actin (detected at 43 kDa) primary polyclonal goat antibody, dilution 1:10,000 (SC-1616) (Santa Cruz, Dallas, TX), was applied. Polyclonal goat anti-rabbit- and rabbit anti-goat-horseradish peroxidase antibodies (DAKO, Copenhagen, Denmark) at dilution 1:10,000 were used as secondary antibodies for target and reference proteins, respectively. ECL *plus* Western Blotting Detection System (Amersham Biosciences, Little Chalfont, UK) was used for protein detection, according to the manufacturer's recommendations. Detection was done using ImageQuant LAS 4000 (GE Healthcare, Little Chalfont, UK). The intensities of bands were quantified using ImageQuant TL (GE Healthcare).

Quantitative reverse transcription-PCR

Complementary DNA was synthesized from 1 µg RNA extracted from cultured fibroblasts as previously described.¹⁴ mRNA amounts using TaqMan assays (Invitrogen, Carlsbad, CA) specific

for DLAT (Hs00898876_m1), DLST (Hs04276516_g1), and DBT (Hs01066445_m1) were measured in triplicates by quantitative real-time PCR using the StepOnePlus detection system (Applied Biosystems, Foster City, CA). Relative gene expression was calculated by the “comparative threshold cycle (C_T) method,” and the expression of the target genes was normalized to the expression of the stably expressed human ACTB (β -actin, 4310881E) (Applied Biosystems) according to the formula: $\Delta C_T = C_T$ (target gene) $- C_T$ (housekeeping gene). Data given are the $2^{-\Delta C_T}$ average ratio of two independent cell-culturing experiments of patient and healthy control cells.

Pyruvate dehydrogenase complex (PDC) activity

PDC activity was analyzed in fibroblast homogenates from healthy controls and patients by a $^{14}\text{CO}_2$ release assay according to ref. ¹⁵. Fibroblasts were grown in Amniochrome Pro medium (Lonza, Basel, Switzerland) supplemented with 150 U/mL penicillin and 30 $\mu\text{g}/\text{mL}$ streptomycin at 37 °C in 5% CO_2 . The cells were homogenized with a Teflon-glass homogenizer in an ice-cold buffer containing 250 mmol/L sucrose, 2 mmol/L EDTA, and 10 mmol/L Tris-HCl pH 7.4. In order to express the PDC activity, citrate synthase activity and protein amount were also determined according to ref. ¹⁵.

RESULTS

Cellular studies in human dermal fibroblasts from three unrelated MCAD-deficient patients (P1–P3) and three healthy controls (C1–C3) were carried out to investigate any differences in the antioxidant response and mitochondrial function. All MCAD-deficient cells were homozygous for the common c.985 A>G *ACADM* variant.

Phenotype in MCADD

Fibroblast cultures derived from MCAD-deficient patients showed significantly higher expression of octanoyl-carnitine (C8) and decanoyl-carnitine (C10) than control fibroblasts. The C8/C10 ratio was approximately sixfold higher in patient fibroblasts compared to healthy control fibroblasts consistent with MCAD deficiency (Fig. 1).

Antioxidant response in MCADD

We examined the level of mitochondrial superoxide in fibroblasts isolated from MCAD-deficient patients and healthy controls by image cytometry using the probe MitoSOX, which is rapidly and

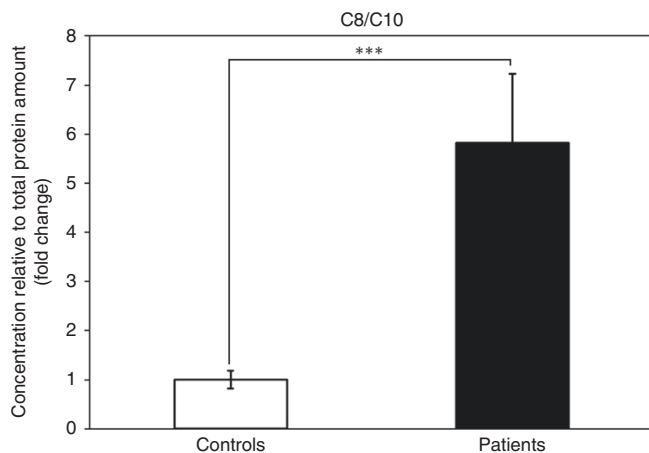


Fig. 1 C8/C10 ratio in fibroblast cultures from healthy controls ($n = 3$) and patients with MCAD deficiency ($n = 3$). Acylcarnitine levels were determined by mass spectrometric analysis and normalized to the total protein amount. The error bars represent standard error of mean (SEM) of three independent experiments, Student’s t test: *** $P < 0.001$.

selectively taken up by mitochondria in the living cells. Patient fibroblasts showed approximately twofold increase in MitoSOX fluorescence intensity compared to the controls (Fig. 2a). The result shows that patient fibroblasts have increased level of mitochondrial ROS compared to control fibroblasts.

The level of LPO was assessed in patient and control fibroblasts by image cytometry using BODIPY, which is a fluorescent probe with good spectral separation of the non-oxidized (595 nm) and oxidized (520 nm) forms. Owing to technical limitations of the NucleoCounter, the oxidized form (green fluorescence) could not be analyzed. Therefore, we used only the decay in the non-oxidized form (orange fluorescence) as a measurement of LPO, which is adequate for this approach and is in line with other technical investigations.¹⁶ MCAD-deficient patient fibroblasts showed significant increase in non-oxidized BODIPY fluorescence intensity (Fig. 2b). The result indicates that the lipids are less oxidatively damaged in fibroblasts from MCAD-deficient patients compared to control fibroblasts. Thus, despite increased mitochondrial ROS, MCADD has less LPO, which could indicate better antioxidant protection. This is consistent with the studies by Zolkipli et al., which show that cultured MCAD-deficient fibroblasts survive an ROS challenge better than healthy controls.¹⁰

We next measured the level of mitochondrial MnSOD to examine the potential response of the mitochondrial antioxidant defense system to the increased level of superoxide. Our data obtained by MS analysis showed that fibroblasts isolated from MCAD-deficient patients display significantly increased MnSOD protein levels amounting to approximately 130% of the MnSOD level in control fibroblasts (Fig. 2c). This is in contrast to short-chain acyl-CoA dehydrogenase (SCAD) deficiency, which exhibits low level of MnSOD protein¹⁴ and decreased survival to an ROS challenge.¹⁰

Mitochondrial function in MCADD

Next, we measured respiration of healthy control and patient fibroblasts using the Seahorse XFe96 extracellular flux analyzer to study the mitochondrial bioenergetics parameters in MCAD deficiency. The schematics of the modified Seahorse XF Cell Mitochondrial Stress Test used in this study are presented in Fig. 3a. OCR of basal respiration of healthy control fibroblasts in each single well (OCR/well) linearly increased with the cell density (Fig. 3b), showing that Seahorse respirometry is applicable for assessing mitochondrial respiratory chain activity within the given range of cell density and allowing normalization of the OCR in each well. No significant differences in OCR rates of ATP-linked respiration, proton leak, and non-mitochondrial respiration between control and patient fibroblasts were observed (data not shown). However, MCAD-deficient cells showed a trend toward increased basal OCR and decreased basal ECAR when compared to control fibroblasts (Fig. 3c, d). Physiologically, mitochondria respire at a submaximal level and maintain a reserve capacity that can be utilized if energy demand is increased. This reserve capacity is calculated as the difference between maximal and basal OCR. The maximal respiration of patient fibroblasts determined after uncoupling mitochondria with FCCP showed 1.5-fold increase in OCR rate compared to the controls (Fig. 3e). In addition, MCAD patient-derived fibroblasts showed approximately twofold increase in OCR rate of reserve capacity compared to the control fibroblasts (Fig. 3f). This reflects increased metabolic flexibility in MCAD-deficient cells and suggests that there is a higher substrate flux capacity through the TCA cycle in MCAD-deficient patient fibroblasts compared to control fibroblasts. Therefore, we set out to study the α -ketoacid dehydrogenase complexes, which in mammalian mitochondria comprise PDC, α -ketoglutarate dehydrogenase (KGDC), and branched-chain α -ketoacid dehydrogenase (BCKDC) multi-enzyme complexes and are responsible for the oxidative decarboxylation of α -ketoacids. These enzymes are key regulators of TCA flux activity and,

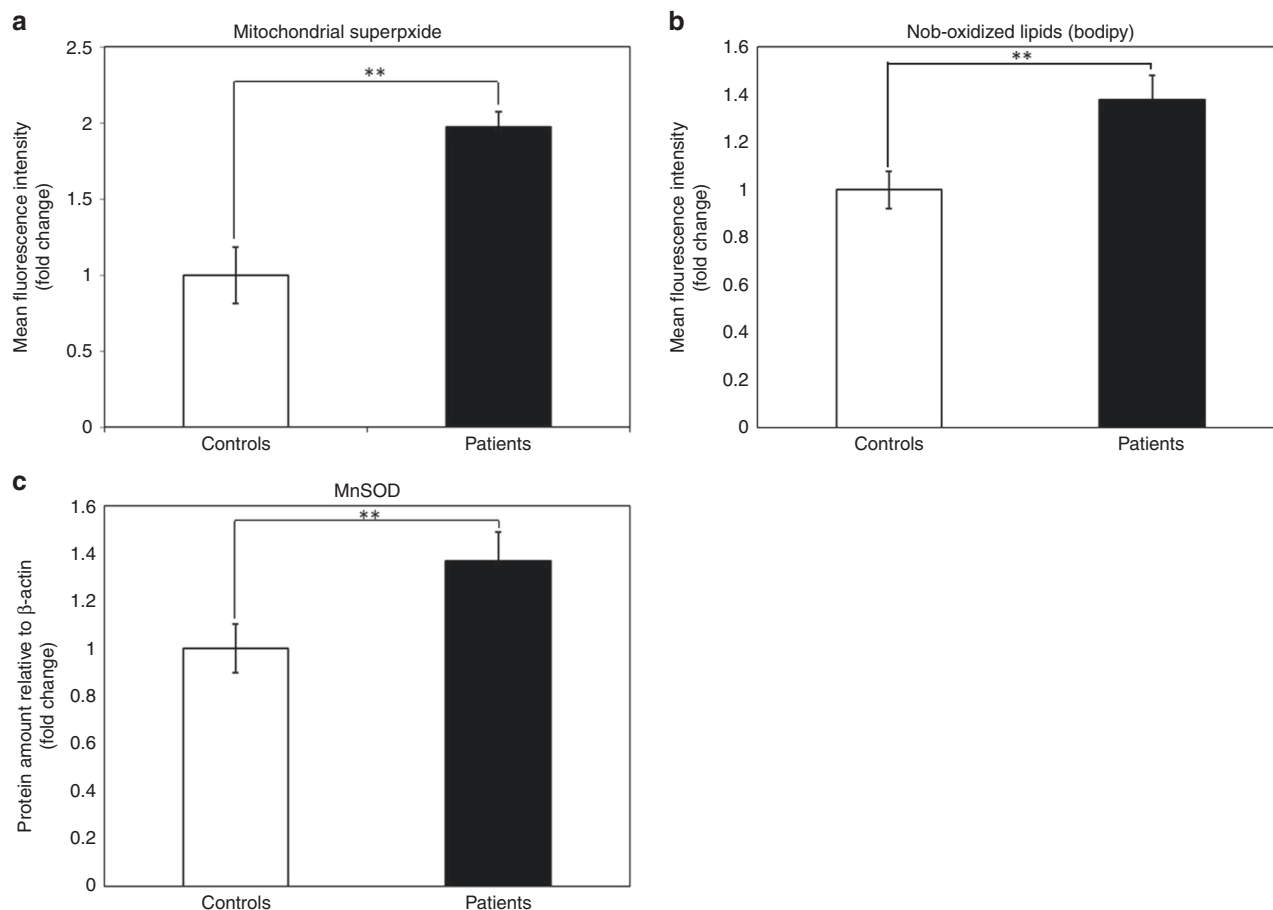


Fig. 2 Oxidative stress and antioxidant response in fibroblast cultures from healthy controls and patients with MCAD deficiency. Level of mitochondrial superoxide (a) and cellular lipid peroxidation (b) were determined by image cytometry using, respectively, mitochondrial superoxide-targeted probe, MitoSOX, and BODIPY probe (non-oxidized form) in fibroblast cultures from patients with MCAD deficiency ($n = 3$) and healthy controls ($n = 3$). Results are expressed as mean fluorescence intensity. Mitochondrial superoxide dismutase (MnSOD) levels (c) were determined by selected reaction monitoring mass spectrometric analysis as described in “Methods” and quantified relative to the β -actin protein amount in fibroblast cultures from patients with MCAD deficiency ($n = 3$) and healthy controls ($n = 3$). The error bars represent standard error of mean (SEM) of two independent experiments, Student’s t test: $**P < 0.01$.

respectively, function in the glycolysis, TCA cycle, and catabolism of valine, leucine, and isoleucine.¹⁷

α -Ketoacid dehydrogenases in MCADD

The protein levels of the three α -ketoacid dehydrogenase complexes were determined by western blot analysis using antibodies directed toward their respective E2 subunits: PDC-E2 (DLAT), BCKDC-E2 (DBT), and KGDC-E2 (DLST) (Fig. 4a). No significant changes were observed in the levels of KGDC-E2 and BCKDC-E2 proteins when comparing MCAD-deficient patient fibroblasts and controls (Fig. 4b, c). However, MCAD-deficient cells displayed significantly increased PDC-E2 protein levels amounting to approximately 380% of the PDC-E2 protein levels in control fibroblasts (Fig. 4a, d).

Lipoic acid is an essential cofactor of the acyltransferase components (E2s) of the α -ketoacid dehydrogenase complexes.¹⁷ E2 contains one or two N-terminal lipoyl subdomains, shuttling the reaction intermediate and reducing equivalents among the active sites of the subunits of the complexes.¹⁷ Lipoic acid is synthesized from octanoic acid,¹⁸ which accumulates in MCAD-deficient cells. Thus it is interesting to speculate that increased protein lipoylation in MCAD-deficient cells may stabilize the activity of α -ketoacid dehydrogenase complexes and improve mitochondrial function. In fact, as compared to controls, MCAD-

deficient cells showed an increase in lipoylated PDC-E2 and KGDC-E2, although the latter did not reach significance due to high variation in protein expression (Fig. 4e, f). Despite using various antibodies, we were not able to detect lipoylated-BCKDC-E2 using western blot analysis. Other studies, investigating lipoylation of α -ketoacid dehydrogenase complexes, have also not been able to detect lipoylated-BCKDC-E2.¹⁹

In order to investigate whether the significant increased protein level of PDC-E2 was caused by a transcriptional regulation, we also analyzed the expression (mRNA level) of the PDC-E2, KGDC-E2, and BCKDC-E2 genes. Our results showed that there was no significant difference between patient and control fibroblasts with regard to the mRNA level of PDC-E2, KGDC-E2, and BCKDC-E2 (Fig. 5), suggesting that increased PDC-E2 protein levels were caused rather by posttranslational lipoylation that may decrease protein turnover by stabilizing the PDC protein itself.

We analyzed also the enzyme activity of PDC to examine the potential higher activity of PDC due to increased level of lipoic acid as the essential cofactor of PDC. No significant difference between fibroblasts isolated from MCAD-deficient patients and healthy controls was observed regardless of whether PDC activity is expressed per mg protein or as a ratio to citrate synthase activity (Fig. 6).

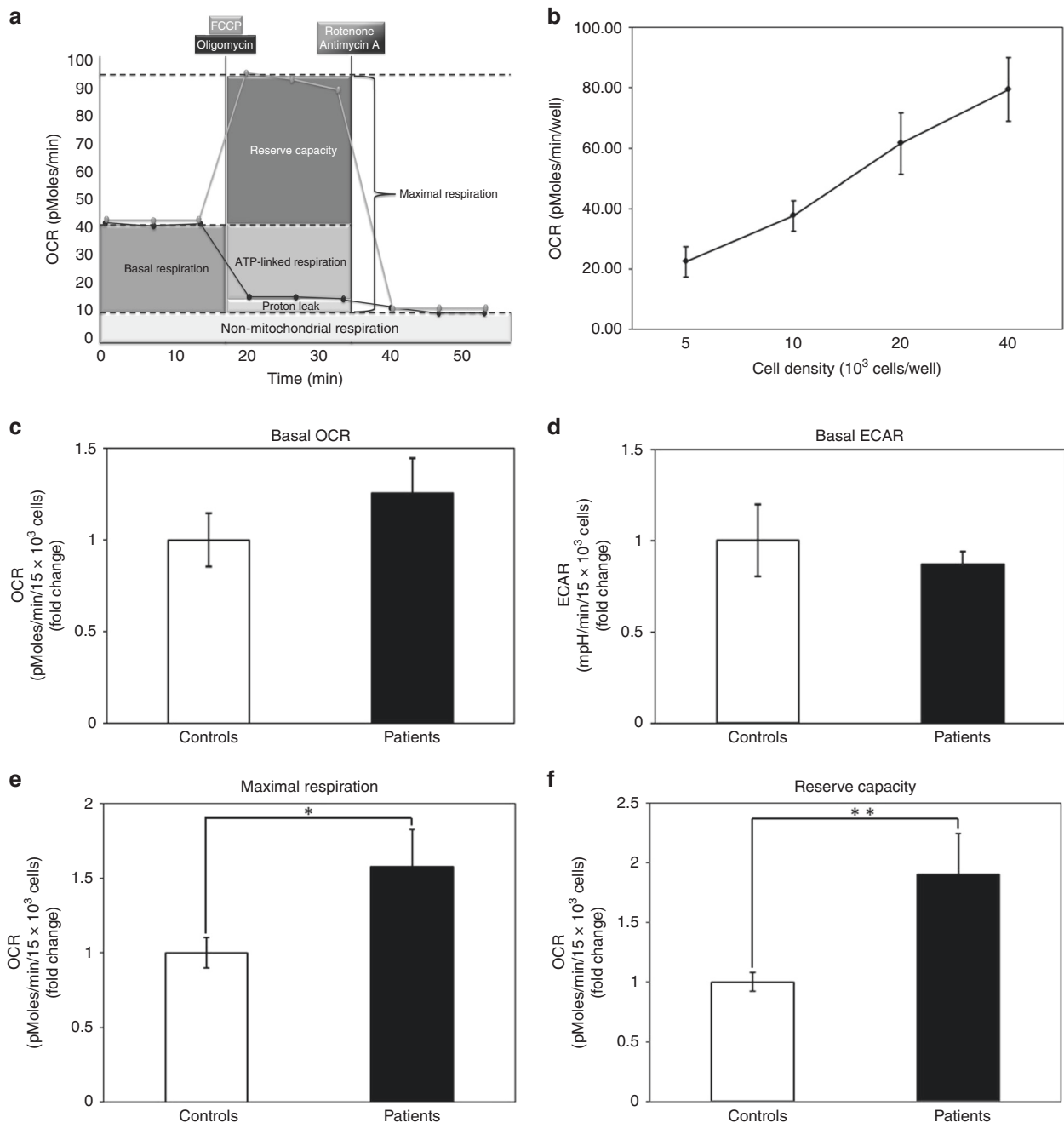


Fig. 3 Mitochondrial bioenergetics profiling of fibroblast cultures from patients with MCADD ($n = 3$) and healthy controls ($n = 3$). Schematic figure of the Seahorse XF Cell Mitochondrial Stress Test. OCR of patient and control fibroblasts was measured in dependence of different mitochondrial respiration inhibitors and uncoupler: (1) Oligomycin (inhibitor of complex V), (2) FCCP (uncoupler) and (3) antimycin A/rotenone (inhibitors of complex I and III, respectively). The reserve capacity was calculated by subtracting the basal OCR from the maximal OCR using the Seahorse technology (a). Linear relationship between the number of cells plated into each microplate well (cell density) and oxygen consumption rate (OCR) of basal respiration in the corresponding wells. Shown are averages of at least 14 measurements for each considered cell density in a single experiment \pm standard deviation (b). OCR and ECAR rates relative to the cell density (15×10^3 cells) for basal OCR (c), basal ECAR (d), maximal respiration (e), and reserve capacity (f). The error bars represent standard error of mean (SEM) of two independent experiments, Student's t test: * $P < 0.05$, ** $P < 0.01$.

DISCUSSION

Zolkipli et al. in 2011 described that MCAD-deficient patient fibroblasts do not have the same degree of increased vulnerability to oxidative stress as seen in other FAO-deficient fibroblasts and control fibroblasts. They showed that fibroblasts from MCAD-deficient patients survived significantly longer compared to other FAO disorders and healthy controls upon menadione-mediated ROS challenge in glucose-containing medium.¹⁰ Therefore, in the

current investigation, we addressed the question of the mechanisms that lead to the protection and longer survival of MCAD-deficient patient fibroblasts compared to control fibroblasts.

The major findings from our study were that MCAD-deficient patient fibroblasts express increased mitochondrial ROS (superoxide anion), but they have less LPO as compared to control fibroblasts. Since LPO is a major mechanism of cellular ROS attack and a stable marker of oxidative stress damage,²⁰ our findings

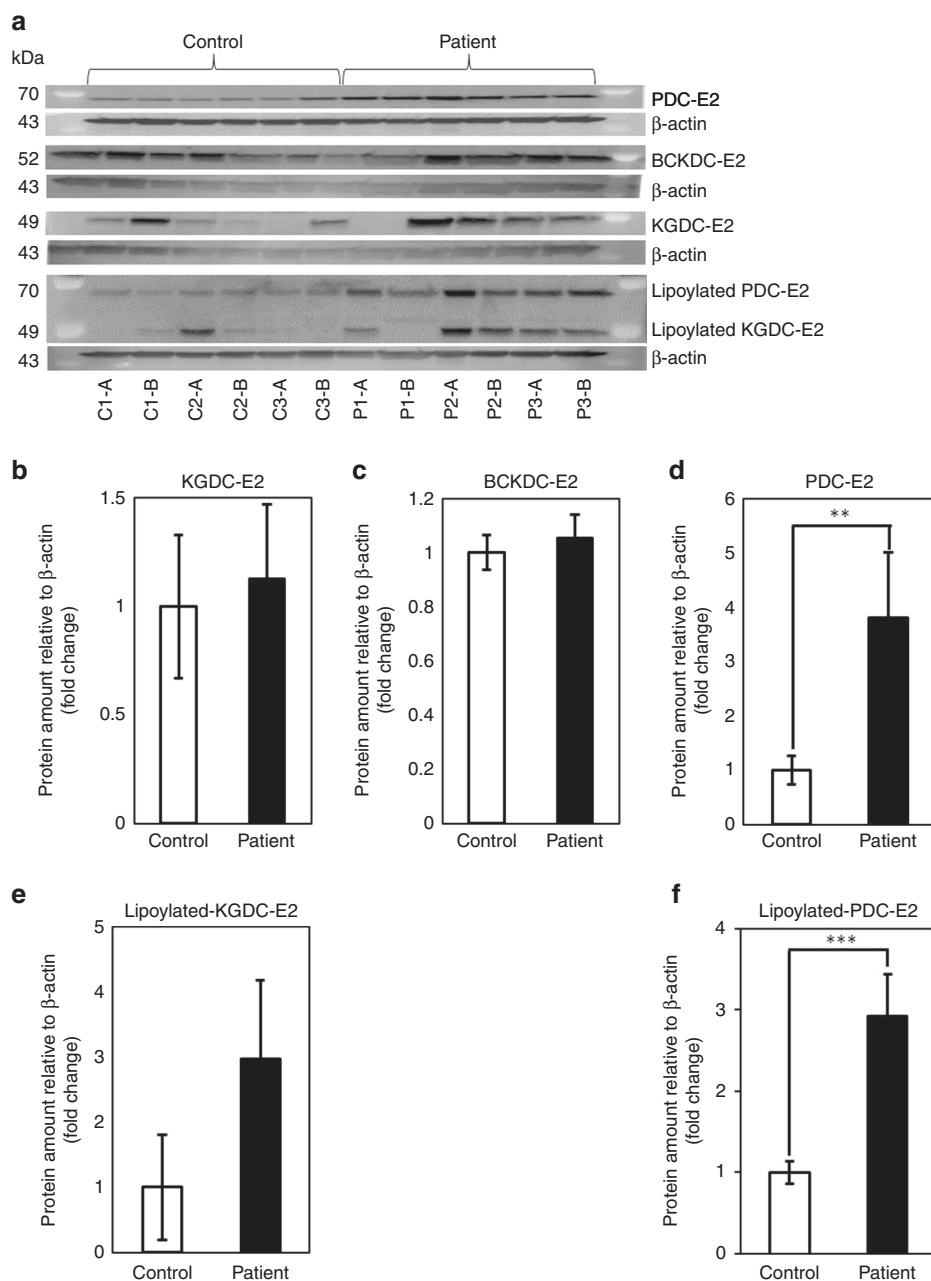


Fig. 4 PDC-E2, KGDC-E2, BCKDC-E2, lipoylated-PDC-E2, and lipoylated-KGDC-E2 protein levels in healthy control and MCAD-deficient patient fibroblasts. The representative western blot of PDC-E2, KGDC-E2, BCKDC-E2, lipoylated-PDC-E2, and lipoylated-KGDC-E2 proteins in control and MCAD-deficient patient fibroblasts; β-actin was used as a loading control (a). Fibroblasts from patients with MCADD ($n = 3$) were analyzed for KGDC-E2 (b), BCKDC-E2 (c), PDC-E2 (d), lipoylated-KGDC-E2 (e), and lipoylated-PDC-E2 (f) protein expression by western blotting and compared to the expression in fibroblasts from healthy controls ($n = 3$). Protein intensities were quantified relative to β-actin protein content. The error bars represent standard error of mean (SEM) of two independent experiments, Student's t test: ** $P < 0.01$, *** $P < 0.001$.

suggest that MCAD-deficient cells have an increased capacity to detoxify mitochondrial ROS. Accordingly, we observed increased mitochondrial antioxidant function, in the form of MnSOD expression, and an increased mitochondrial glucose oxidation capacity, as reflected by the increased PDC-E2 and lipoylated PDC-E2 protein amounts, accompanied by an increased mitochondrial maximal respiration and increased reserve capacity, all of which have been linked to increased cell survival in the presence of oxidative stress stimuli.^{21,22} Based on these findings, we raise the interesting hypothesis that increased PDC-bound lipoic acid, synthesized from accumulated octanoic acid in MCADD, may affect the cellular antioxidant pool in MCADD.

Cellular ROS detoxification and mitochondrial substrate oxidation is tightly linked.^{23,24} During acute or mild increases in ROS, glucose uptake and oxidation is increased, and this is protective against ROS-induced cell death. Mechanistically, this protection could be due to oxidative redox activation of AMPK (adenosine monophosphate-activated protein kinase) or Nrf2 (nuclear factor, erythroid 2 like 2), which induce coordinated expression of cellular antioxidant systems and metabolic flux, needed for supporting their activity.^{25,26} Among the expressed genes are MnSOD, which rapidly converts superoxide anion, produced as a natural by-product of mitochondrial electron transport, into hydrogen peroxide. Hydrogen peroxide is then detoxified to water utilizing

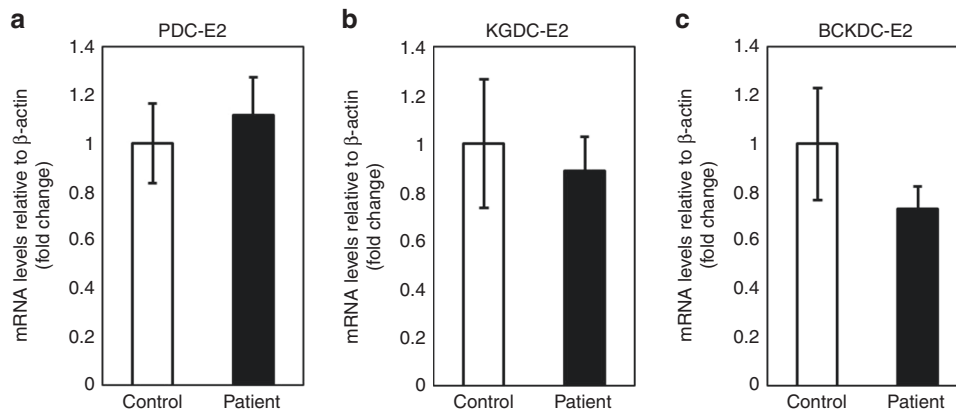


Fig. 5 Expression of PDC-E2, KGDC-E2, and BCKDC-E2 genes in healthy control and MCAD-deficient patient fibroblasts. mRNA level of PDC-E2 (a), KGDC-E2 (b), and BCKDC-E2 (c) genes, measured relative to β -actin by RT-qPCR in fibroblast cultures from patients with MCADD ($n = 3$) and healthy controls ($n = 3$). The error bars represent standard error of mean (SEM) of two independent experiments.

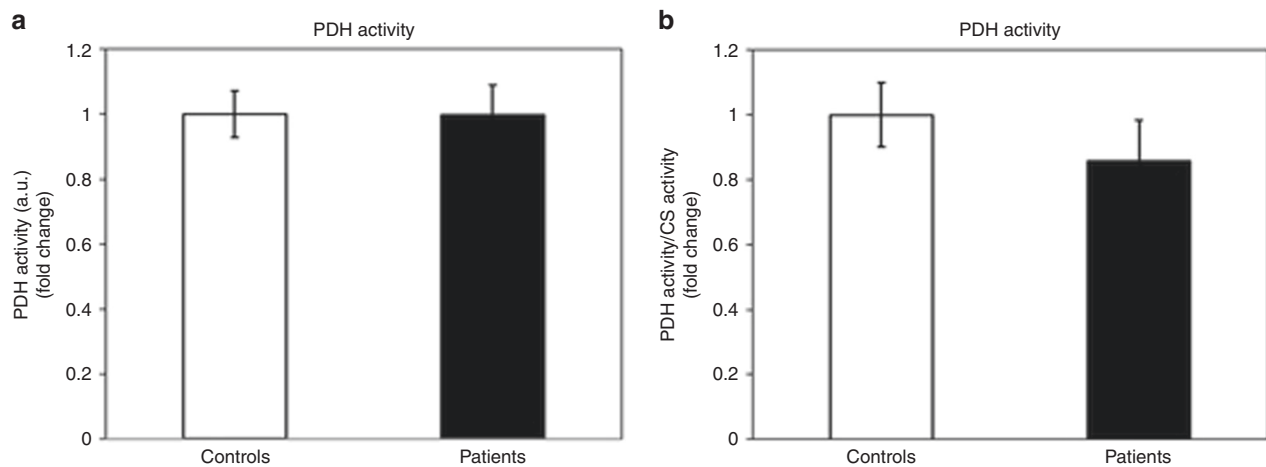


Fig. 6 Pyruvate dehydrogenase activity in healthy control ($n = 3$) and MCAD-deficient patient ($n = 3$) fibroblasts expressed per mg protein (a) and as a ratio to citrate synthase activity (b). The error bars represent standard error of mean (SEM) of one measurement in duplicate.

glutathione or thioredoxin/peroxiredoxin redox couples, whose reduction is driven by the common electron donor NADPH, the generation of which is dependent on an active TCA cycle.

Our data showed that MCAD-deficient cells have increased PDC-E2 expression and a tendency toward increased OCR and decreased ECAR, reflecting that MCAD-deficient fibroblasts are shifted more toward glucose oxidation than toward glycolytic lactate production as compared to controls. Similar, Ventura et al. showed that cultured fibroblast cells, derived from MCAD-deficient patients, produce less lactate when compared to both healthy control fibroblasts and to fibroblasts from patients with very long-chain acyl-CoA dehydrogenase (VLCAD) deficiency or long-chain 3-hydroxyacyl-CoA dehydrogenase (LCHAD) deficiency.²⁷ Differences in glucose metabolism is also evidenced clinically by the fact that lactic acidosis is a common finding in patients with long-chain FAO disorders but is rarely seen in patients with MCAD deficiency.^{28,29} In accordance with their decreased glucose oxidation, MnSOD has been shown to be downregulated in long-chain FAO disorders with elevated mitochondrial superoxide anion and chronic oxidative stress, such as VLCAD deficiency, LCHAD deficiency, and riboflavin-responsive multiple acyl-CoA dehydrogenation deficiency,^{30,31} and also in SCAD-deficient patient fibroblasts.¹⁴ SCAD-deficient cells as well as cells with long-chain FAO deficiency also showed decreased survival upon an oxidative stress challenge as compared to MCAD-

deficient cells.¹⁰ In contrast, SOD is increased in MCAD-deficient patients as evidenced from the present cell study and a clinical study by Derks and co-workers.⁶ So data from this and other studies support that antioxidant function in FAO disorders depend on mitochondrial glucose oxidation. Moreover, while these mechanisms are activated in MCAD-deficient cells, they are lost in long-chain FAO disorders. Accordingly, the ability of MCAD-deficient cells to tolerate ROS better than healthy controls was lost when the cells were cultured without glucose.¹⁰

These different cellular responses may reflect chronic adaptive remodeling to different amounts of ROS produced as a consequence of the primary gene defect in the cells. ROS are hormetins that follow a biphasic response curve, where cellular antioxidant function is stimulated at low doses but inhibited at high doses.^{24,32} In fact, long-chain acyl-CoA esters inhibit ETC activity and increase oxidative stress to a larger extent than medium-chain acyl-CoA esters,³³ suggesting that less ROS are released from the ETC in MCAD-deficient cells as compared to long-chain FAO cells.

Another interesting hypothesis could be that the increased PDC-bound lipoic acid, synthesized from accumulated octanoic acid in MCAD-deficient cells, may allow sufficient glucose oxidation and NADPH availability to keep hydrogen peroxide within its hormetic zone for activation of cellular antioxidant systems. Even though the present study did not show any

regulation in PDC activity under basal conditions, the increased availability of lipoylated PDC-E2 may enable prompt posttranslational enzyme activation during stress, as reflected in the present study by the immediate increase in maximal respiration and reserve capacity upon mitochondrial uncoupling by FCCP in MCAD-deficient cells as compared to healthy controls. Thus the reduction in LPO in MCAD-deficient cells, as compared to healthy controls, could in part be attributable to increased levels of PDC-E2-bound lipoic acid in mitochondria, which is in line with other investigations, demonstrating that lipoic acid improves glucose oxidation^{34,35} and provides protection against 4-hydroxy-2-nonenal, the most studied of the cytotoxic products of LPO.³⁶

In human cells, the lipoate cofactor is assembled on its apo-protein using octanoate from mitochondrial fatty acid synthesis, and very little lipoate exists as the free acid.³⁷ We speculate that octanoate, when accumulated in high amounts as in MCAD-deficient cells, can directly be converted into protein-bound lipoate, similar to what has been observed in bacteria.³⁸ Notably, endurance exercise increases the protein-bound lipoyl lysine pool in the liver and skeletal muscles and improves mitochondrial function,³⁹ suggesting that endogenous lipoate synthesis takes place in situations where high-energy demands overwhelm the capacity of FAO. In fact, we did find increases in lipoylated PDC-E2 and lipoylated KGDC-E2 in MCAD-deficient cells as compared to controls, although the increase in KGDC-E2 did not reach significant levels, perhaps due to one lipoyl-binding domain in KGDC-E2 as compared to two lipoyl-binding domains in PDC-E2.¹⁷ However, while it is an interesting theory that accumulated octanoic acid in MCAD-deficient cells can increase E2-bound lipoic acid and thereby glucose oxidation and overall TCA cycle activity, it is also possible that increased E2-bound lipoic acid, similar to increased MnSOD, reflects upregulation of the cellular antioxidant system as a response to mild oxidative stress and is not necessarily a specific feature of MCAD-deficient cells. Clearly, a more comprehensive analysis of lipoate-dependent dehydrogenases and detailed investigations of lipoic acid synthesis and regulation in MCAD-deficient cells are needed to clarify its possible antioxidant role in MCAD-deficient cells.

Among the known disorders of mitochondrial FAO, MCAD deficiency is by far the most mild one. When properly diagnosed and appropriately treated to prevent hypoglycemic episodes, most patients are able to live an asymptomatic life.⁵ VLCAD and SCAD may partly compensate for insufficient MCAD enzyme activity, since they have an overlap of substrate specificity.¹ While this has been put forward to explain the relatively mild phenotype in MCAD deficiency, oxidative stress have also been suggested to play an important role in disease pathogenesis.^{6–9} Based on data presented in this study, we have argued that the oxidative stress in MCAD deficiency is milder than seen in other FAO disorders and suggested that increased level of PDC-E2-bound lipoic acid, produced from accumulated octanoic acid, or as a possible secondary response to mild oxidative stress in MCAD-deficient cells, may increase respiratory reserve capacity and improve the ability of MCAD-deficient cells to resist metabolic changes and oxidative stress. While more studies are necessary to pinpoint why MCAD-deficient patients are more protected against oxidative stress compared to other FAO disorders and healthy controls, data presented in this study have implications for our understanding of how glucose availability contribute to MCAD-deficiency pathogenesis, not only as an alternative energy source during limited FAO activity but also as an important regulator of cellular antioxidant function.

ACKNOWLEDGEMENTS

We thank the Faculty of Health Sciences at Aarhus University and the Danish Council for Independent Research (Grant Nos. #4004-00548 and #11-107331) for financial support.

AUTHOR CONTRIBUTIONS

Z.N.: experimental design, performed the experiments, data analysis, and writing the first draft of the manuscript. R.I.D.B.: performed the mass spectrometric analysis. P.F.-G.: MitoSOX and lipid peroxidation data analysis, set up the Seahorse profile protocol, and revised the manuscript. J.H.: performed the acylcarnitine analysis and revised the manuscript. 5. F.W.: performed the pyruvate dehydrogenase activity measurement. T.J.C.: experimental design, report editing, and revising the manuscript. N.G. and R.K.J.O.: experimental design, report editing, data analysis, and critically revising the manuscript.

ADDITIONAL INFORMATION

Competing interests: The authors declare no competing interests.

Publisher's note Springer Nature remains neutral with regard to jurisdictional claims in published maps and institutional affiliations.

REFERENCES

- Gregersen, N. et al. Mitochondrial fatty acid oxidation defects—remaining challenges. *J. Inherit. Metab. Dis.* **31**, 643–657 (2008).
- Gregersen, N., Bross, P. & Andresen, B. S. Genetic defects in fatty acid beta-oxidation and acyl-CoA dehydrogenases. Molecular pathogenesis and genotype-phenotype relationships. *Eur. J. Biochem.* **271**, 470–482 (2004).
- Tanaka, K. et al. A survey of the newborn populations in Belgium, Germany, Poland, Czech Republic, Hungary, Bulgaria, Spain, Turkey, and Japan for the G985 variant allele with haplotype analysis at the medium chain acyl-CoA dehydrogenase gene locus: clinical and evolutionary consideration. *Pediatr. Res.* **41**, 201–209 (1997).
- Bross, P. et al. Effects of two mutations detected in medium chain acyl-CoA dehydrogenase (MCAD)-deficient patients on folding, oligomer assembly, and stability of MCAD enzyme. *J. Biol. Chem.* **270**, 10284–10290 (1995).
- Andresen, B. S. et al. MCAD deficiency in Denmark. *Mol. Genet. Metab.* **106**, 175–188 (2012).
- Derks, T. G. et al. Experimental evidence for protein oxidative damage and altered antioxidant defense in patients with medium-chain acyl-CoA dehydrogenase deficiency. *J. Inherit. Metab. Dis.* **37**, 783–789 (2014).
- Lim, S. C. et al. Loss of the mitochondrial fatty acid beta-oxidation protein medium-chain acyl-coenzyme A dehydrogenase disrupts oxidative phosphorylation protein complex stability and function. *Sci. Rep.* **8**, 153 (2018).
- Scaini, G. et al. Toxicity of octanoate and decanoate in rat peripheral tissues: evidence of bioenergetic dysfunction and oxidative damage induction in liver and skeletal muscle. *Mol. Cell. Biochem.* **361**, 329–335 (2012).
- Schuck, P. F. et al. Medium-chain fatty acids accumulating in MCAD deficiency elicit lipid and protein oxidative damage and decrease non-enzymatic antioxidant defenses in rat brain. *Neurochem. Int.* **54**, 519–525 (2009).
- Zolkipli, Z., Pedersen, C. B., Lamhonwah, A. M., Gregersen, N. & Tein, I. Vulnerability to oxidative stress in vitro in pathophysiology of mitochondrial short-chain acyl-CoA dehydrogenase deficiency: response to antioxidants. *PLoS ONE* **6**, e17534 (2011).
- Fernandez-Guerra, P. et al. Application of an image cytometry protocol for cellular and mitochondrial phenotyping on fibroblasts from patients with inherited disorders. *JIMD Rep.* **27**, 17–26 (2016).
- Zhou, Y. et al. Mitochondrial spare respiratory capacity is negatively correlated with nuclear reprogramming efficiency. *Stem Cells Dev.* **26**, 166–176 (2017).
- Birkler, R. I., Nochi, Z., Gregersen, N. & Palmfeldt, J. Selected reaction monitoring mass spectrometry for relative quantification of proteins involved in cellular life and death processes. *J. Chromatogr. B Anal. Technol. Biomed. Life Sci.* **1035**, 49–56 (2016).
- Pedersen, C. B. et al. Antioxidant dysfunction: potential risk for neurotoxicity in ethylmalonic aciduria. *J. Inherit. Metab. Dis.* **33**, 211–222 (2010).
- Ostergaard, E. et al. Four novel PDHA1 mutations in pyruvate dehydrogenase deficiency. *J. Inherit. Metab. Dis.* **32**(Suppl 1), S235–S239 (2009).
- Drummen, G. P., Makkinje, M., Verkleij, A. J., Op den Kamp, J. A. & Post, J. A. Attenuation of lipid peroxidation by antioxidants in rat-1 fibroblasts: comparison of the lipid peroxidation reporter molecules cis-parinaric acid and C11-BODIPY(581/591) in a biological setting. *Biochim. Biophys. Acta* **1636**, 136–150 (2004).
- Perham, R. N. Swinging arms and swinging domains in multifunctional enzymes: catalytic machines for multistep reactions. *Annu. Rev. Biochem.* **69**, 961–1004 (2000).
- Mayr, J. A., Feichtinger, R. G., Tort, F., Ribes, A. & Sperl, W. Lipoic acid biosynthesis defects. *J. Inherit. Metab. Dis.* **37**, 553–563 (2014).

19. Tort, F. et al. Mutations in the lipoyltransferase LIPT1 gene cause a fatal disease associated with a specific lipoylation defect of the 2-ketoacid dehydrogenase complexes. *Hum. Mol. Genet.* **23**, 1907–1915 (2014).
20. Ayala, A., Munoz, M. F. & Arguelles, S. Lipid peroxidation: production, metabolism, and signaling mechanisms of malondialdehyde and 4-hydroxy-2-nonenal. *Oxid. Med. Cell. Longev.* **2014**, 360438 (2014).
21. Hill, B. G., Dranka, B. P., Zou, L., Chatham, J. C. & Darley-Usmar, V. M. Importance of the bioenergetic reserve capacity in response to cardiomyocyte stress induced by 4-hydroxynonenal. *Biochem. J.* **424**, 99–107 (2009).
22. Nickens, K. P., Wikstrom, J. D., Shirihai, O. S., Patierno, S. R. & Ceryak, S. A bioenergetic profile of non-transformed fibroblasts uncovers a link between death-resistance and enhanced spare respiratory capacity. *Mitochondrion* **13**, 662–667 (2013).
23. Liemburg-Apers, D. C., Willems, P. H., Koopman, W. J. & Grefte, S. Interactions between mitochondrial reactive oxygen species and cellular glucose metabolism. *Arch. Toxicol.* **89**, 1209–1226 (2015).
24. Olsen, R. K., Cornelius, N. & Gregersen, N. Redox signalling and mitochondrial stress responses; lessons from inborn errors of metabolism. *J. Inherit. Metab. Dis.* **38**, 703–719 (2015).
25. Rabinovitch, R. C. et al. AMPK maintains cellular metabolic homeostasis through regulation of mitochondrial reactive oxygen species. *Cell Rep.* **21**, 1–9 (2017).
26. Heiss, E. H., Schachner, D., Zimmermann, K. & Dirsch, V. M. Glucose availability is a decisive factor for Nrf2-mediated gene expression. *Redox Biol.* **1**, 359–365 (2013).
27. Ventura, F. V., Ruiter, J. P., IJ, L., de Almeida, I. T. & Wanders, R. J. Lactic acidosis in long-chain fatty acid beta-oxidation disorders. *J. Inherit. Metab. Dis.* **21**, 645–654 (1998).
28. lafolla, A. K., Thompson, R. J. Jr. & Roe, C. R. Medium-chain acyl-coenzyme A dehydrogenase deficiency: clinical course in 120 affected children. *J. Pediatrics* **124**, 409–415 (1994).
29. Jackson, S. et al. Long-chain 3-hydroxyacyl-CoA dehydrogenase deficiency. *Pediatr. Res.* **29**, 406–411 (1991).
30. Tonin, A. M. et al. Long-chain 3-hydroxy fatty acids accumulating in LCHAD and MTP deficiencies induce oxidative stress in rat brain. *Neurochem. Int.* **56**, 930–936 (2010).
31. Cornelius, N., Corydon, T. J., Gregersen, N. & Olsen, R. K. Cellular consequences of oxidative stress in riboflavin responsive multiple acyl-CoA dehydrogenation deficiency patient fibroblasts. *Hum. Mol. Genet.* **23**, 4285–4301 (2014).
32. Olsen, R. K., Cornelius, N. & Gregersen, N. Genetic and cellular modifiers of oxidative stress: what can we learn from fatty acid oxidation defects? *Mol. Genet. Metab.* **110**(Suppl), S31–S39 (2013).
33. Wang, B. et al. Effects of long-chain and medium-chain fatty acids on apoptosis and oxidative stress in human liver cells with steatosis. *J. Food Sci.* **81**, H794–H800 (2016).
34. Estrada, D. E. et al. Stimulation of glucose uptake by the natural coenzyme alpha-lipoic acid/thioctic acid: participation of elements of the insulin signaling pathway. *Diabetes* **45**, 1798–1804 (1996).
35. Khanna, S., Roy, S., Packer, L. & Sen, C. K. Cytokine-induced glucose uptake in skeletal muscle: redox regulation and the role of alpha-lipoic acid. *Am. J. Physiol.* **276**, R1327–R1333 (1999).
36. Korotchkina, L. G., Yang, H., Tirosh, O., Packer, L. & Patel, M. S. Protection by thiols of the mitochondrial complexes from 4-hydroxy-2-nonenal. *Free Radic. Biol. Med.* **30**, 992–999 (2001).
37. Cao, X., Zhu, L., Song, X., Hu, Z. & Cronan, J. E. Protein moonlighting elucidates the essential human pathway catalyzing lipoic acid assembly on its cognate enzymes. *Proc. Natl Acad. Sci. USA* **115**, E7063–E7072 (2018).
38. Booker, S. J. Unraveling the pathway of lipoic acid biosynthesis. *Chem. Biol.* **11**, 10–12 (2004).
39. Khanna, S. et al. Skeletal muscle and liver lipoyllysine content in response to exercise, training and dietary alpha-lipoic acid supplementation. *Biochem. Mol. Biol. Int.* **46**, 297–306 (1998).